Received: 7 January 2020 | Accepted: 3 April 2020
DOI: 10.1002/pros.23985

ORIGINAL ARTICLE

The Prostate WILEY

Interaction between prostate cancer cells and prostate fibroblasts promotes accumulation and proteolytic processing of basement membrane proteins

Marjaana Ojalill PhD[1] | Noora Virtanen MSc[1] | Pekka Rappu PhD[1] | Elina Siljamäki PhD[1] | Pekka Taimen MD, PhD[2] | Jyrki Heino MD, PhD[1]

[1]Department of Biochemistry, University of Turku, Turku, Finland

[2]Department of Pathology, Turku University Hospital, University of Turku, Turku, Finland

Correspondence
Jyrki Heino, Department of Biochemistry, University of Turku, Finland.
Email: jyrki.heino@utu.fi

Funding information
K. Albin Johanssons Stiftelse; Academy of Finland, Grant/Award Number: 259769; Sigrid Juséliuksen Säätiö; European Commission, Grant/Award Numbers: Marie Curie ITN, CAFFEIN; Syöpäjärjestöt

Abstract

Background: Tumor microenvironment or stroma has the potency to regulate the behavior of malignant cells. Fibroblast-like cells are abundant in tumor stroma and they are also responsible for the synthesis of many extracellular matrix components. Fibroblast-cancer cell interplay can modify the functions of both cell types.

Methods: We applied mass spectrometry and proteomics to unveil the matrisome in 3D spheroids formed by DU145 prostate cancer cells, PC3 prostate cancer cells, or prostate-derived fibroblasts. Similarly, DU145/fibroblast and PC3/fibroblast coculture spheroids were also analyzed. Western blot analysis and immunofluorescence were used to confirm the presence of specific proteins in spheroids. Cancer dissemination was studied by utilizing "out of spheroids" migration and invasion assays.

Results: In the spheroid model cancer cell-fibroblast interplay caused remarkable changes in the extracellular matrix and accelerated the invasion of DU145 cells. Fibroblasts produced structural matrix proteins, growth factors, and matrix metalloproteinases. In cancer cell/fibroblast cocultures basement membrane components, including laminins (α3, α5, β2, and β3), heparan sulfate proteoglycan (HSPG2 gene product), and collagen XVIII accumulated in a prominent manner when compared with spheroids that contained fibroblasts or cancer cells only. Furthermore, collagen XVIII was intensively processed to different endostatin-containing isoforms by cancer cell-derived cathepsin L.

Conclusions: Fibroblasts can promote carcinoma cell dissemination by several different mechanisms. Extracellular matrix and basement membrane proteins provide attachment sites for cell locomotion promoting adhesion receptors. Growth factors and metalloproteinases are known to accelerate cell invasion. In addition, cancer cell-fibroblast interplay generates biologically active fragments of basement membrane proteins, such as endostatin.

KEYWORDS
ECM, endostatin, fibroblasts, invasion, laminin-332, prostate cancer

1 | INTRODUCTION

Malignant tumors contain several nontransformed cell types, including endothelial cells, various inflammatory cells, and fibroblasts.[1] Cancer cells as well as all other cell types in tumors are surrounded by extracellular matrix (ECM). ECM is an insoluble scaffold for cells and at the same time a reservoir of matrix-bound growth factors, which has the ability to alter malignant cell behavior.[2] ECM in the tumor stroma is mainly synthesized by fibroblast-like cells, often by a special group of activated mesenchymal cells, called cancer-associated fibroblasts (CAFs).[3] In prostate cancer fibroblasts become activated before the actual malignant growth, at the prostate intraepithelial neoplasia stage.[4] In vitro coculture of stromal cells together with cancer cells has been used to study cell behavior in tumor-like circumstances. CAFs' contribution to the cancer cell motility has been shown to be mediated by secreted growth factors[5,6] or by CAF-modified aligned matrix.[7-9] Many studies have reported abnormal composition, organization, or stiffness of the ECM in malignant tumors.[4,8,10-12] Tumor progression and resistance to therapy can partially be connected to altered ECM architecture or biochemical properties.[13-16] In addition, ECM can be modulated by degradation, posttranslational modification or de novo synthesis of matrix proteins.[1] Many proteases, including matrix metalloproteinases (MMPs), mediate the degradation of ECM and consequently reorganize the matrix and release matrix-derived bioactive peptides.[17] It is well acknowledged that CAFs release growth factors and bioactive protein fragments that can regulate cancer cell division and invasion.[6] Most often CAFs have been connected to the promotion of tumor growth,[7-9,18,19] but inhibition of tumor progression has been reported as well.[20]

The aim of the present study was to determine how direct prostate cancer cell-prostate fibroblast interaction modulates tumor stroma and cell invasion. The study included "out of spheroid" invasion assays and mass spectrometry analysis of the ECM proteins. Our results show that the interplay between prostate fibroblasts with DU145 or PC3 cells in 3D spheroid cocultures leads to remarkable changes in the composition of ECM and concomitantly to the accelerated invasion of the prostate cancer cells.

2 | MATERIALS AND METHODS

2.1 | Cell culture

The human androgen-independent prostate epithelial adenocarcinoma cell lines DU145 and PC3 (both from American Type Culture Collection) and human prostate-derived fibroblastic cells, described previously[21] were cultured in Roswell Park Memorial Institute (RPMI)-1640 medium (Lonza), supplemented with 10% fetal calf serum (FCS, Biowest), 2 mM Ultraglutamate, 100 U/mL penicillin and streptomycin (Lonza). In the indicated experiments also serum-free (SF) RPMI-1640 medium or keratinocyte serum-free medium (KSFM) with 5 ng/mL human recombinant epidermal growth factor, 50 μg/mL bovine pituitary extract (Gibco), supplemented with 2 ng/mL recombinant human leukemia inhibitory factor and 2 ng/mL stem cell factor (Sigma Aldrich) was used. Cells were routinely screened with MycoAlert PLUS *Mycoplasma* detection kit (Lonza).

2.2 | Spheroid cultures

Spheroids were made in micro-molds according to the manufacturer's instructions (3D Petri Dish, MicroTissues) and they contained either only one cell line or both cancer cells and CAFs. Monoculture spheroids contained 1.4×10^5 cells in one mold (4000 cells/spheroid) and cocultures 2.8×10^5 cells in one mold (4000 cancer cells and 4000 CAFs/spheroid). Spheroids were grown in RPMI-1640 SF media. Cathepsin L inhibitor (Z-FY-CHO, Santa Cruz Biotechnology) in the concentrations of 10 μM and 50 μM or equal amount of dimethyl sulfoxide (DMSO) for control was added daily to spheroid medium to study the proteolytic degradation of ECM proteins.

2.3 | Spheroid intensity profiling

The spheroid intensity profiles obtained from ImageJ were aligned by normalizing the distances from the spheroid edge by spheroid diameter. The original intensity values and spheroid diameter were determined from a single z-stack (the middle stack of all the z-stacks) of confocal images by using the plot profile tool in ImageJ. For each channel separately, the aligned intensities were normalized by the total area under the intensity curve. 15 spheroids from three independent biological replicates were analyzed.

2.4 | Immunofluorescence and confocal microscopy

Before spheroids were made cancer cells were stained with Cell Tracker Green (CMFDA, 5 μM, Invitrogen) and fibroblasts with Orange (CMTMR, 5 μM, Invitrogen) for 1 hour to distinct cancer cells and CAFs from each other during imaging. After staining cells were allowed to recover 30 minutes with fresh growth media, thereafter trypsinized and spheroids were prepared as explained above. Cells were let to grow for 72 hours, then fixed with 4% paraformaldehyde-phosphate-buffered saline (PBS), 3 hours, +4°C, stained with 4′,6-diamidino-2-phenylindole, and mounted with glycerol.

2.5 | Migration and invasion assay

Cells were seeded into micro-molds to form spheroids for 72 hours as explained above. Three different conditions were used: first, media were not changed; second media were changed daily and it contained either 50 μg/mL ascorbic acid; or contained 1 mM hydroxyurea as third option. Thereafter spheroids were transferred from molds to

96-well plate coated with Collagen I 5 μg/cm^2 o/n at +4°C and blocked with 0.1% bovine serum albumin (BSA)-PBS 1 hour at +37°C. In migration study KSFM was added on top of the spheroid. In invasion study Collagen I gel was first added on top of the spheroid and KSFM was added into the wells after gel was properly formed. Spheroids were imaged every 24 hours for 4 days by using IncuCyte ZOOM System. To study the effects of MMP inhibition on the cells invasion medium was supplemented with 1 μM NNGH (Sigma) or 10 μM NSC 405020 (Sigma) with respectively amount of DMSO as control.

2.6 | Sample preparation for mass spectrometry

Spheroids were collected and treated o/n at +4°C with hypotonic lysis buffer (HLB) containing (10 mM Tris, 1 mM EDTA, and 10 μg/mL DNAse) to release soluble cytoplasmic proteins. The next day samples were washed two times with HLB and centrifuged between washes at 12 600 g and +4°C for 2.5 minutes. Samples were recovered by centrifugation as mentioned above and dissolved in solution containing 8 M urea and 100 mM ammonium bicarbonate. The cysteine was reduced by 10 mM diothiotreitol at +37°C for 2 hours and alkylated in 40 mM iodoacetamide for 30 minutes. Iodoacetamide was inactivated by increasing dithiothreitol concentration to 30 mM. Proteins were digested with trypsin/Lys C-mixture (Promega) first for 4 hours at +37°C so that trypsin/Lys C-mixture added was 1/50 of the protein concentration. Urea concentration was decreased to 0.6 M and ammonium bicarbonate concentration was increased to 80 nM to reactivate trypsin. Trypsin/Lys C-mixture concentration was increased to 1/25 of the protein concentration and incubated overnight at +37°C. The peptides were desalted by StageTips and loaded on a nanoflow high-performance liquid chromatography system (Easy-nLCII, Thermo Fisher Scientific) coupled to the QExactive mass spectrometer (Thermo Fisher Scientific) equipped with a nano-electrospray ionization source. Three repeated runs per sample were performed. Information about mass spectrometry runs and details of proteomics data analysis can be found in Supplementary Methods. The mass spectrometry proteomics data are available through the ProteomeXchange Consortium via the PRIDE repository with the data set identifier PXD016882.

2.7 | Western blot analysis

Cells grown as spheroids for 6 days with a daily change to fresh media (RPMI with 0% FCS, 50 μg/mL ascorbic acid) were treated with HLB as explained in the mass spectrometry section. The protein pellet was suspended into radioimmunoprecipitation assay buffer (Thermo Fisher Scientific). The 6 × sodium dodecyl sulfate (SDS) sample buffer was added and samples were boiled 5 minutes at 100°C. Protein aliquots were separated in 6% to 15% SDS-polyacrylamide gel electrophoresis gels, thereafter proteins were immobilized onto polyvinylidene difluoride-membrane. The following primary antibodies were used: laminin-5 (ab14509, Abcam); endostatin (PA1-601, Thermo Fisher Scientific); MMP-14 (AB6005, Sigma-Aldrich), and β-actin (A-1978, Sigma-Aldrich). The membranes were incubated with the primary antibodies overnight at +4°C, followed by incubation with secondary antibodies (680RD or 800CW; 926-32213, 926-32212, 926-68072, or 926-68073, LI-COR Biosciences) in 5% BSA in Tris-buffered saline with Tween-20 for 1 hour at room temperature. Odyssey CLx from Li-COR Biosciences was used to detect fluorescent bands on membrane, band intensities were analyzed with Image Studio program (LI-COR) and protein expressions were shown as relative to β-actin.

2.8 | Adhesion assay

Cell adhesion was measured in real time with xCelligence technology (Acea Biosciences Inc.). DU145 cells (10 000/well) were seeded on 96-well xCelligence E-plate (Acea Biosciences Inc) coated with fibronectin (Sigma, 5 μg/cm^2 in PBS, +4°C, overnight), blocked with 1% BSA in PBS (+37°C, 1 hour). As a control BSA treated wells were used. When indicated human recombinant Endostatin (PeproTech Inc, 40 μg/mL) was added to the SF media prior plating the cells. Cell spreading was followed for 20 hours with xCelligence RTCA (Acea Biosciences Inc). For statistical analysis three different experiments were combined and cell adhesion difference between fibronectin and fibronectin with endostatin in the media was calculated at 1 hour 30 and 10 hours time points.

2.9 | Statistical analysis

The paired two-sample Student *t* tests, One way analysis of variance with Tukey or Dunnett T3 post hoc tests were performed by using IBM SPSS Statistics software version 22.

3 | RESULTS

3.1 | Prostate fibroblasts modify the cellular organization and the composition of ECM in spheroid cocultures with PC3 and DU145 prostate cancer cell

We used mass spectrometry and proteomics to analyze the composition of ECM in the spheroids formed by DU145 or PC3 prostate cancer cells or by their cocultures with prostate-derived fibroblasts. Without fibroblasts DU145 and PC3 cells produced a very limited number of matrisome and matrisome-associated proteins. Totally 64 proteins were recognized and most of them were ECM-regulators (32.8%), ECM-affiliated proteins (25%), or secreted factors (20.3%) (Figure 1A). Thirty-two out of 64 proteins were produced by both cell lines, while DU145 had four and PC3 28 unique gene products (Figure 1B; Table SI). None of the common or DU145-specific gene

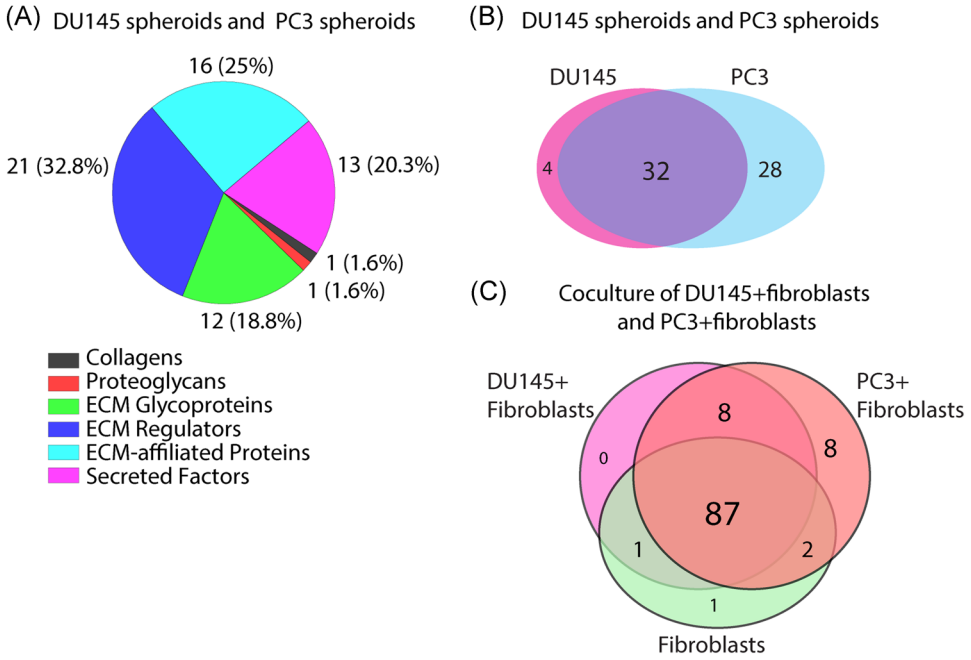

FIGURE 1 Cancer cells produce limited number of core matrisome proteins. A, Most of the proteins identified from DU145 and PC3 spheroid culture matrices in mass spectrometry analysis fall into the categories of ECM regulators, ECM-affiliated proteins and secreted factors. Only one protein from groups of collagens and proteoglycans was identified. B, Prostate cancer cell lines share 32 matrix proteins out of 64; DU145 cells exclusively synthesize four matrix proteins and are unable to synthesize matrix structural proteins. PC3 cells synthesize 28 proteins not identified in DU145 cells, these include laminins, HSGP2, and collagen type VI (Table SI). C, The majority of matrisome proteins are synthesized by fibroblasts. About 87 proteins were shared between fibroblasts only, DU145/fibroblasts, and PC3/fibroblasts matrisomes. ECM, extracellular matrix [Color figure can be viewed at wileyonlinelibrary.com]

products represented core matrisome structural proteins, while PC3 cells could produce laminin chains α3, β3, γ2, as well as HSPG2 and collagen VI (COL6A1) (Figure 1B; Table SI). In accordance with our previous observations,[21] fibroblastic cells were responsible for the production of the structural proteins in the core matrisome (Figure 1C; Table 1). The major components of collagenous, fibronectin-rich ECM could be detected in fibroblast spheroids, including the two α chains of fibril forming collagen I (COL1A1 and COL1A2), fibril-associated proteins, such as collagen XII (COL12A1) and decorin (DCN), tenascin C (TNC), and beaded filament-forming collagen VI (COL6A2 and COL6A3) (Table 1). Prostate-derived fibroblasts also produced MMPs, since MMP-14 (also called membrane type 1 metalloproteinase, MT1-MMP) was recognized in the samples. Comparison of matrisome profiles in fibroblast, DU145/fibroblast, and PC3/fibroblast spheroids revealed remarkable similarity, that is, 87 out of 107 proteins identified (Figure 1C).

In cancer cell/fibroblast cocultures basement membrane components, such as laminins (α3, α5, β2, and β3), heparan sulfate proteoglycan (HSPG2 gene product), and collagen XVIII accumulated in a more prominent manner when compared with spheroids that contained one cell type only (Table 2). Proteoglycans agrin and syndecan 4 had enhanced expression in the cocultures, too (Table 2). The increased accumulation of these proteins was observed in both PC3/fibroblast and DU145/fibroblast spheroids. At the same time, the interplay between prostate cancer cells and fibroblasts led to a diminished accumulation of a number of ECM proteins, most notably fibrillin-2 (FBN2), fibulin-1 (FBLN1), and collagen XIV (Table 2).

Staining of fibroblasts and cancer cells with distinct Cell Trackers unveiled organization of the 5 days old coculture spheroids. Confocal z-stack mode images and maximum projection were used to get an overview of the cellular localization. In the majority of DU145/fibroblast spheroids the fibroblasts surrounded the core formed by DU145 cells. In contrast, in PC3/fibroblast spheroids the two cell types were mixed, that is, the similar fibroblastic capsule was not formed and the surface of the spheroid was often covered by PC3 cells (Figure 2A,B).

3.2 | Cancer cell-fibroblast interaction promotes proteolytic processing of basement membrane components

To confirm the mass spectrometry results we performed Western blots utilizing specific antibodies to laminin-332 (previously called laminin-5) and to endostatin, a protein derived from the C-terminal part of collagen XVIII. These analyses indicated that all three laminin subunits in laminin-332, namely, α3, β3, and γ2, were upregulated in cancer cell/fibroblast coculture spheroids (Figure 3). Importantly, it was also possible to see lower molecular mass bands (~40 kDa), which suggested proteolytic processing of laminin (Figure 3). Similarly, in

TABLE 1 Matrisome proteins synthesized by fibroblasts

Only by fibroblasts
HGF
FBLN1
COL12A1
TNFAIP6
COL14A1
LTBP1/LTBP2
MMP14
LAMB1
WNT5A
VWA5A
FGF2
COL6A2
IGFBP5
LEPREL2
COL1A1
FBN1
COL6A3
EMILIN1
NID2
PXDN
COL15A1
COL1A2
COL3A1
PLOD1
FN1
LAMC1
COL4A1
HTRA1
COL4A2
DCN
TGFBI
PLAT
TNC

Abbreviations: COL1, collagen I; COL3, collagen III; COL4, collagen IV; COL6, collagen VI; COL12, collagen XII; COL14, collagen XIV; COL15, collagen XV; DCN, decorin; FBLN1, fibulin-1; FGF2, fibroblast growth factor 2; HGF, hepatocyte growth factor; LTBP, latent-transforming growth factor beta-binding protein; MMP14, metalloproteinase 14; TGFBI, transforming growth factor beta induced; TNC, tenascin C; TNFAIP6, tumor necrosis factor-inducible gene 6 protein.

DU145/fibroblast spheroids collagen XVIII was intensively processed to ~30 kDa endostatin-containing fragment (Figure 4A,B), a common degradation product in a process also generating the classical ~20 kDa endostatin.[22] The potential role of endostatin in DU145–ECM interaction was also tested using real time xCelligence technology to measure cell attachment and spreading on ECM protein fibronectin-coated surfaces. Human recombinant endostatin was shown to significantly promote the adhesion of DU145 cells to fibronectin (Figure 4C,D). To conclude these results, the spheroids contained proteolytic activity that could modify the basement membrane-associated proteins and generate their functional fragments, which also have the capability to regulate cancer cell behavior.

The presence of MMP-14 in both DU145/fibroblast and PC3/fibroblast coculture spheroids was confirmed in Western blot experiments (Figure S1A). In further experiments two MMP inhibitors were used: NNGH (N-isobutyl-N-(4-methoxyphenylsulfonyl) glycyl hydroxamic acid), a selective inhibitor of MMP-3 and a broad spectrum inhibitor of many MMPs, and NSC 405020, a selective inhibitor of MMP-14/MT1-MMP. However, MMP inhibitors could not significantly prevent the formation of either endostatin-related proteins (Figure S1B,C) or laminin fragments (Figure S1D). Thus in spheroids proteinases other than MMPs seem to be responsible for the proteolytic degradation of these basement membrane components. Based on our mass spectrometric analysis DU145 and PC3 cells express several cathepsins, namely cathepsin B, D, L, and Z (Table SI). Cathepsin L has been shown to release endostatin from collagen XVIII NC1-domain.[22] Accordingly, in our coculture spheroids a selective Cathepsin L inhibitor (Z-FY-CHO) in a concentration of 50 μM significantly decreased the formation of ~30 kDa endostatin-containing protein (Figure 5).

3.3 | Interplay between DU145 cells and fibroblasts promotes the motility of cancer cells in 3D invasion model

In cancer the invasion of malignant cells leads to the local progression of the disease and later to the formation of metastases. Both DU145 and PC3 are considered to represent invasive cell phenotypes.[23] Here, we established an invasion assay that measures the ability of cells to move out of the coculture spheroid. At first, prostate cancer cells or prostate-derived fibroblasts or both cell types together were allowed to form spheroids. After 72 hours in culture these spheroids were placed on collagen I coated surfaces or inside collagen I gels. Migration on collagen I or invasion through collagen I gel was followed by phase-contrast microscopy for 96 hours. Fibroblasts alone did not invade out from the spheroids (Figure 6A-E). In this experimental setting PC3 cells in coculture with fibroblasts invaded into the collagen gel less effectively than DU145 cells (Figure S2) and, therefore, the following experiments were performed with DU145 and DU145/fibroblast spheroids only.

In 2D conditions, cell migration out of DU145 spheroids was more efficient when compared with DU145/fibroblast spheroids (Figure 6A). However, invasion of cells inside 3D collagen gels was significantly faster when DU145/fibroblast spheroids were assayed and compared with spheroids solely formed by either DU145 cells or fibroblasts (Figure 6B). When DU145 cells and fibroblasts were differentially

TABLE 2 Matrisome proteins enriched in fibroblast/cancer cell coculture

Protein names	Gene names	FC DU145 + fibroblasts vs sum of DU145 and fibroblasts	FC PC3 + fibroblasts vs sum of PC3 and fibroblasts
Tubulointerstitial nephritis antigen-like	*TINAGL1*	138.2	4.7
Laminin subunit alpha-5	*LAMA5*	25.3	5.4
Basement membrane-specific heparan sulfate proteoglycan core protein	*HSPG2*	7.6	3.7
Laminin subunit beta-2	*LAMB2*	5.8	3.0
Galectin-3	*LGALS3*	4.9	3.0
Agrin	*AGRN*	4.1	2.6
Laminin subunit beta-3	*LAMB3*	3.6	4.0
Syndecan-4	*SDC4*	3.3	2.3
Laminin subunit alpha-3	*LAMA3*	3.2	3.5
Collagen alpha-1(XVIII) chain; endostatin	*COL18A1*	2.8	5.2
Serine protease HTRA1	*HTRA1*	2.0	2.4
Protein S100-A8	*S100A8*	ND	39.4
Protein S100-A9	*S100A9*	ND	14.8
Fibroblast growth factor-binding protein 1	*FGFBP1*	ND	10.0
Elafin	*PI3*	ND	7.0
Antileukoproteinase	*SLPI*	ND	3,4
Deleted in malignant brain tumors 1 protein	*DMBT1*	Infinity	−7.8
Fibrillin-2	*FBN2*	−6.3	−10.4
Fibulin-1	*FBLN1*	−4.7	−8.1
Collagen alpha-1(XIV) chain	*COL14A1*	−5.5	−5.7
Cathepsin Z	*CTSZ*	−2.0	−3.4
Annexin A4	*ANXA4*	−4.2	−3.2
Lysosomal protective protein	*CTSA*	−2.0	−3.0
Annexin A6	*ANXA6*	−4.7	−2.0
Latent-transforming growth factor beta-binding protein 1	*LTBP1*	−14.6	−2.0
Tumor necrosis factor-inducible gene 6 protein	*TNFAIP6*	−Infinity	−6.3
Hepatocyte growth factor	*HGF*	−Infinity	−Infinity

Note: Infinity/−Infinity, not detected in one side of comparison.
Abbreviations: FC, fold change; ND, not detected.

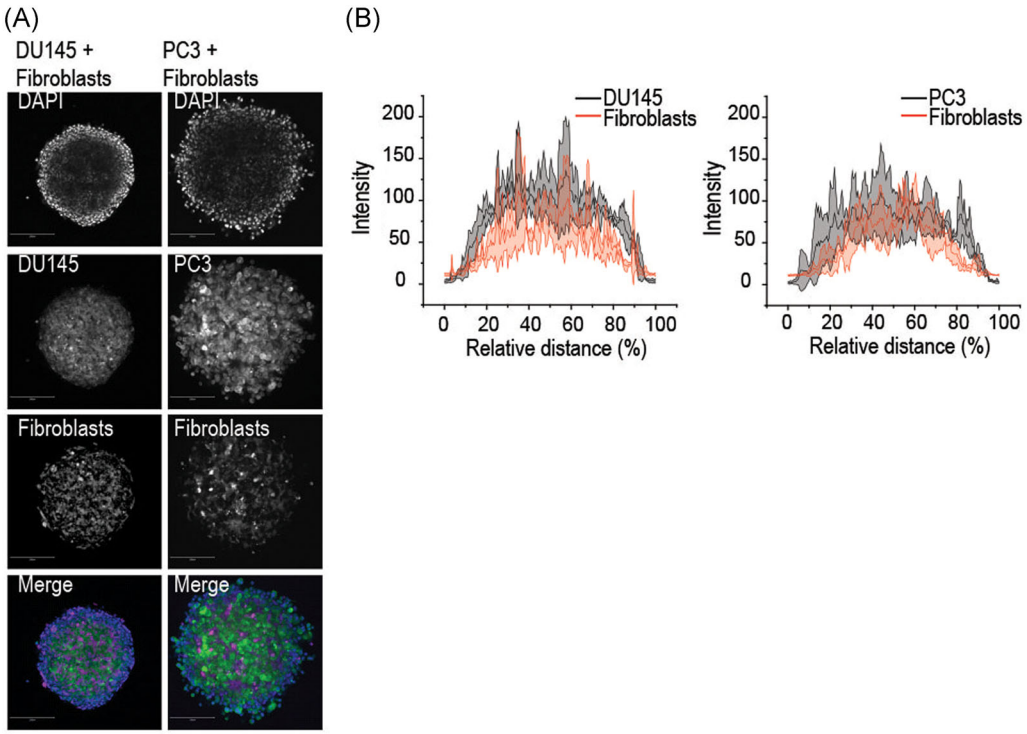

FIGURE 2 A distinct cancer cell location in spheroids: fibroblasts surround the DU145 cells creating tight spheroids, whereas PC3 cells also locate on the edges of spheroid and fibroblasts in middle creating more incompact spheroids. A, Representative images of cancer cells and fibroblasts grown in spheroids for 96 hours shown as maximum intensity projections. DU145 and PC3 cells were stained with Cell Tracker Green (CMFDA, Invitrogen) and fibroblasts with Orange (CMTMR, Invitrogen), nuclei were stained with DAPI. Bar 200 μm. B, Quantification of expression profiles of cancer cells (black line) and fibroblasts (red line) indicating the localization in spheroids. The cells were treated as in (A), and the expression profile was calculated from the confocal images. Mean intensity values show the intensities of cancer cells (black) and fibroblasts (red), and relative distance indicates the diameter of the spheroids. 15 spheroids from three biological replicates were analyzed. Mean (the middle dark line) ± SEM (light area around the middle line) is shown. DAPI, 4′,6-diamidino-2-phenylindole [Color figure can be viewed at wileyonlinelibrary.com]

stained with Cell Trackers, it was obvious that already after 24 hours DU145 was the invading cell type, while most fibroblasts stayed in spheroids (Figure 6C). To ensure that the difference in invasion was not affected by cell number, experiments in which hydroxyurea was used to block cell proliferation were performed. The inhibition of cell growth had no effects on the invasion (Figure 6D).

These results suggest that in spheroids fibroblasts activate DU145 cells and initiate invasion. In the presence of ascorbic acid, the difference between DU145/fibroblast and DU145 spheroids remained the same (Figure 6E), which suggests that triple helical collagens produced by the fibroblasts or organization of the collagenous matrix is not part of the mechanism how fibroblasts support cancer motility. DU145 cells can use direct integrin α2β1-mediated adhesion to collagen I.[24] It is also possible that basement membrane protein production induced by fibroblasts in DU145 cells has a positive effect on an invasion. However, it is not clear, whether in these conditions DU145 cells are able to take full advantage of ECM produced by fibroblasts. In addition soluble factors, for example, growth factors or MMPs, produced by fibroblasts may play part in the process. Indeed, we could detect hepatocyte growth factor (HGF) and fibroblast growth factor (FGF2) in spheroid cultures (Table 1).

To test the potential role of MMPs during the invasion process we used the two selective inhibitors, NNGH and NSC 405020, as above. Both inhibitors could significantly inhibit the migration and invasion of DU145 cells (Figure 7A,B), but a similar phenomenon could also be seen in the absence of fibroblasts (Figure 7A,B). Taken together, our data show that the presence of fibroblasts in the microenvironment enhances cancer cell dissemination possibly through several mechanisms.

4 | DISCUSSION

Tumor stroma is an important regulator of cancer progression. We applied 3D cell culture methods to study the effects of stromal fibroblasts on ECM production and cell invasion in prostate tumors. In spheroid cultures prostate fibroblasts could produce, in addition to the basic ECM components, many classical basement membrane proteins, including laminin chains β1 (LNB1) and γ1 (LNC1), collagen IV (COL4A1 and COL4A2), and basement membrane-associated proteins fibulin-1 (FBLN1) and collagen XV (COL15A1). However, accumulation of several basement membrane proteins was only seen

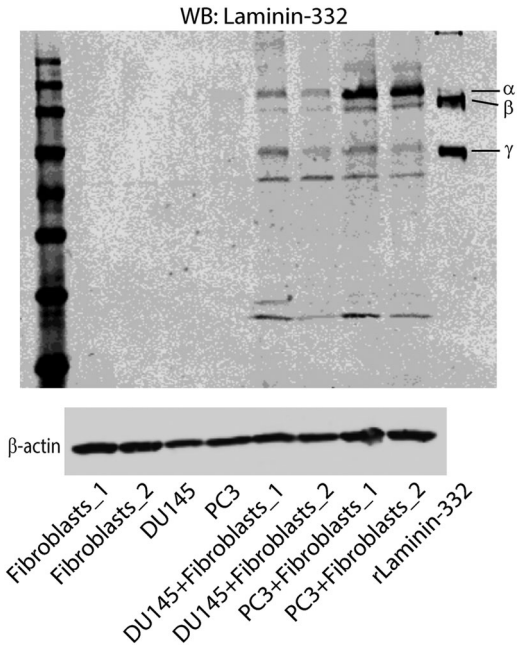

FIGURE 3 Coculturing of prostate fibroblasts with DU145 or PC3 cancer cells induces synthesis of basement membrane component laminin-332 and its active degradation. Representative Western blot analysis of laminin-332 expression. Cells grown as spheroids were allowed to produce ECM for 6 days, thereafter, cells were lyzed and matrix proteins collected for WB analysis. Human recombinant laminin-332 was used as positive control. ECM, extracellular matrix

in cancer cell/fibroblast cocultures. These gene products included α3, α5, β2, β3 laminins, heparan sulfate proteoglycan (HSPG2 gene product), and collagen XVIII.

Incompletely organized, thin basement membranes as well as the down regulation of α6β4 integrin and other hemidesmosome-associated proteins are typically seen in prostate cancer.[25,26] One earlier report suggests that the expression of LN332 related gene products (α3, β3, and γ2) is lost, whereas the corresponding messenger RNA levels have paradoxically elevated.[27] Here, our results propose that the in vivo activation of laminin genes may be due to the interplay of cancer cells with stromal fibroblasts. Based on our observations, in addition to LN332 also the expression of other laminins can be induced in such circumstances, since the detected laminin gene products have the potency to form also other trimers, such as LN321, LN521, LN522, and LN523. Recently, it was shown that the interplay between fibroblasts and cutaneous squamous cell carcinoma cells resulted in the accumulation of laminin-332 in a H-Ras- and TGF-β signaling dependent manner, which consequently enhanced motility of cancer cells.[28] However, in prostate cancer Ras mutations are rather infrequent.[29] Furthermore, the simultaneous activation of proteolytic processes may explain the disappearance of laminin LN332 proteins. Importantly, laminin degradation products may enhance cell mobility.[30]

Degradation of collagen XVIII to endostatin was another indication of the active proteolysis of basement membrane-related proteins in spheroid cultures. Endostatin is well known about its

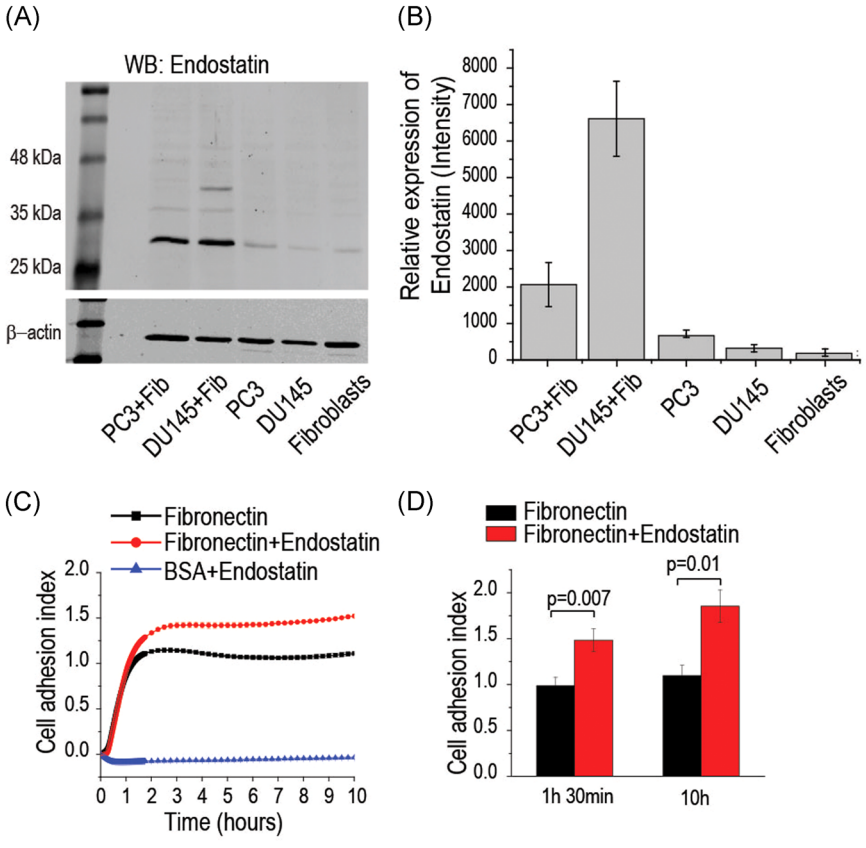

FIGURE 4 Coculturing of prostate fibroblasts with DU145 or PC3 cancer cells induce degradation of basement membrane component Collagen XVIII into endostatin-containing fragments. A, The representative Western blot analysis of endostatin expression in DU145 or PC3 cells alone or cocultured with fibroblasts. B, The quantification of endostatin expression in DU145 or PC3 cells cultured alone or cocultured with fibroblasts (n = 3). C, Representative cell adhesion assay of DU145 cells binding and spreading on fibronectin with (red line) and without (black line) added endostatin measured with Xcelligence system. D, Quantification of DU145 cells attachment to fibronectin was significantly increased in the presence of endostatin (40 μg/ml) at 90 minutes and 10 hour time points. n = 3, $P < .05$ by Student t test. BSA, bovine serum albumin [Color figure can be viewed at wileyonlinelibrary.com]

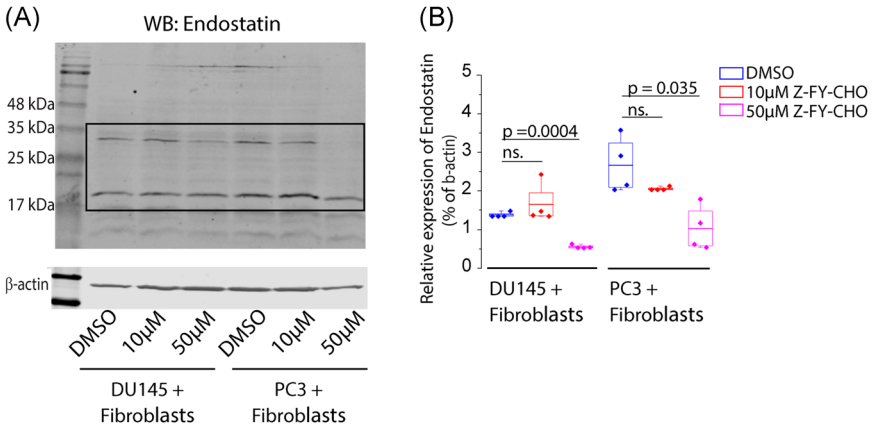

FIGURE 5 Cathepsin L inhibitor decreases the formation of endostatin-containing fragments in DU145 and PC3 co-cultures with fibroblasts. A, Representative Western blot analysis of endostatin expression in DU145 or PC3 cells cocultured with fibroblasts in the presence of DMSO (control) or cathepsin L inhibitor at 10 μM or 50 μM concentration. B, The quantification of cathepsin L inhibitor effect on expression of 30 kDa endostatin-containing fragment in co-cultures of DU145 or PC3 cells with fibroblasts (n = 4), $P < .05$ by one way ANOVA with Dunnett T3 post hoc test. ANOVA, analysis of variance; DMSO, dimethyl sulfoxide [Color figure can be viewed at wileyonlinelibrary.com]

antiangiogenic properties.[31] The effects of endostatin on endothelial cell proliferation, migration, and apoptosis have also been reported in various cancer cells.[32-36] Interestingly, in prostate cancer cells endostatin can also regulate androgen receptor function.[37] Here, our results indicate that endostatin promotes the adhesion of DU145 cells to fibronectin. Thus it is a potential regulator of adhesion-related functions of prostate cancer cells.

ECM proteins can be degraded by several proteases, including serine proteases, cathepsins, which are cysteine proteases, and MMPs. Here, in spheroid cultures fibroblasts produced detectable amounts of membrane-type metalloproteinase MMP-14, known to be able to degrade multiple ECM proteins, including LN332. Furthermore, we could also find one member of the trypsin family of serine proteases, namely, HTRA1 to be expressed by fibroblasts. In addition to fibroblast-derived enzymes, DU145 and PC3 cells produced cathepsins D, B, L, and Z, and PC3s also cathepsin C. Thus, the proteolytic processing of ECM proteins is promoted by both cancer cells and fibroblasts.

The proteolytic process leading to the generation of endostatin from collagen XVIII is still poorly understood. MMP-14 is one of the MMPs that can generate endostatin from collagen XVIII,[38] but our experiments utilizing MMP inhibitors showed that in DU145/fibroblast cocultures MMP-14 is not responsible for either endostatin or laminin fragment formation. In previous studies secreted cathepsin L has been indicated to be one of the key enzymes in the process leading to the generation of endostatin.[22] In our spheroid model a selective inhibitor of cathepsin L significantly decreased the formation of 30 kDa endostatin-containing fragment. Thus the presence of this cancer cell-derived cysteine proteinase may at least partially explain the processing of fibroblast-derived collagen XVIII to endostatin. Interestingly, in many cancers, the overexpression of cathepsins has been connected to the worse prognosis and more invasive phenotype of carcinoma.[39]

Invasion is one of the hallmark properties of cancer cells. In our experiments, the close contact between fibroblasts and DU145 in spheroids stimulated the invasion by DU145 cells, whereas fibroblasts mainly stayed in spheroids. In addition to changes in ECM composition fibroblasts may also promote invasion by the production of growth factors, since in spheroid cultures we were able to detect HGF and FGF2. Interestingly, in colon cancer, HGF and TGF-β synergistically stimulate laminin γ2 chain expression.[40]

5 | CONCLUSIONS

To conclude, our results suggest that prostate fibroblasts can promote prostate cancer cell invasion by several simultaneous mechanisms. Fibroblasts produce the majority of components of ECM around the cancer cells and the interplay between fibroblasts and cancer cells induces the expression of many basement membrane proteins. Together, the two cell types synthesize a mixture of proteolytic enzymes that have the capability to promote cell invasion and to generate biologically active peptides derived from the basement membrane proteins. Furthermore, fibroblasts produce soluble regulators, such as growth factors, that activate cancer cells. In general, our observations stress the importance of prostate cancer cell-prostate fibroblast interaction in the process that leads the dissemination of the disease and present 3D spheroid cocultures as an adequate model to study tumor microenvironment.

ACKNOWLEDGMENTS

We thank the Academy of Finland, the Sigrid Juselius Foundation, the Finnish Cancer Associations, K. Albin Johansson Foundation, and the 7th framework program of European Union (Marie Curie INT, CAFFEIN). We are grateful for obtaining patient tissue material from Pathology Department of University of Turku and from Auria

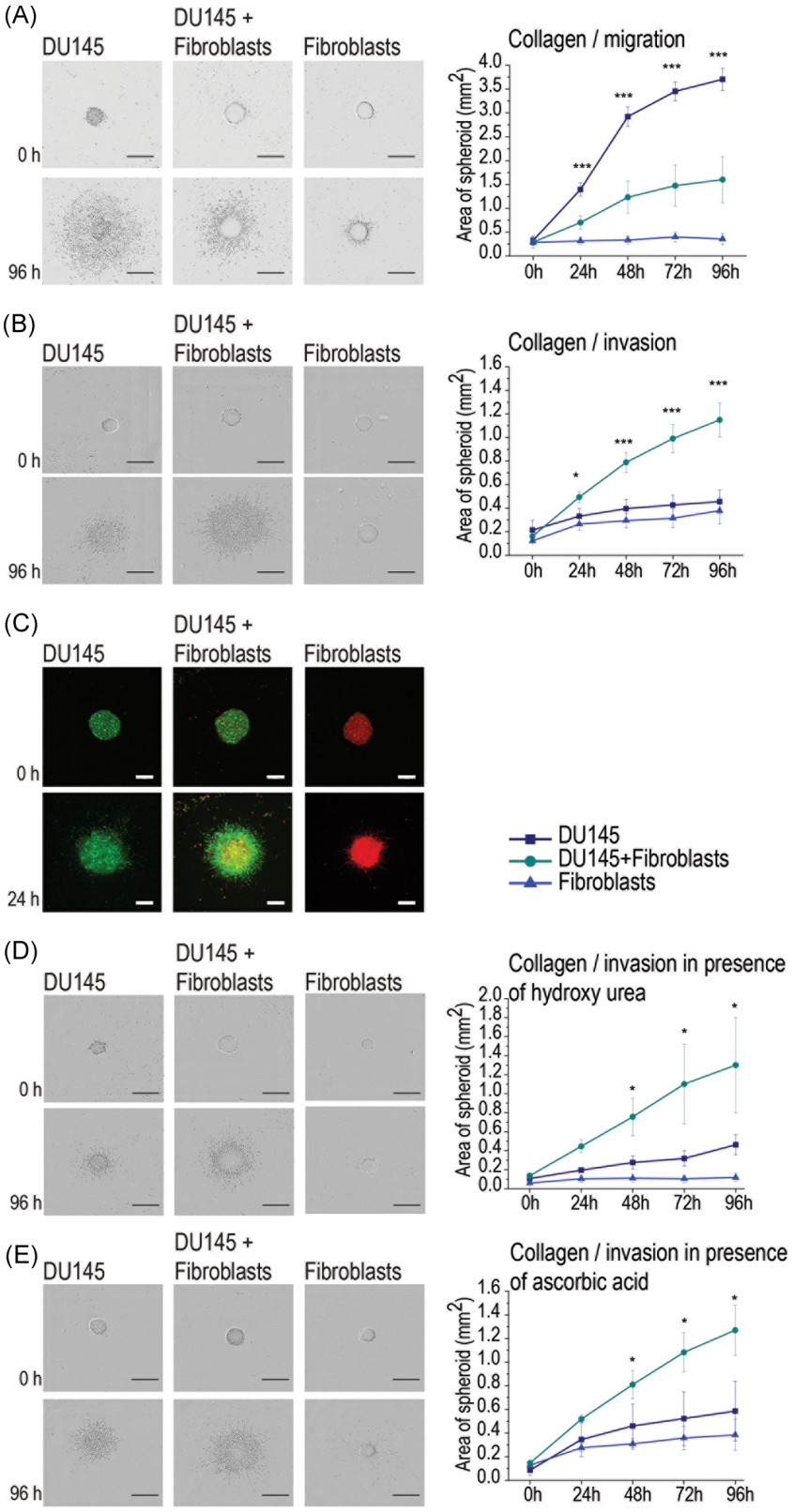

FIGURE 6 Fibroblasts induce invasion capability of DU145 cancer cells in coculture. A, Representative images and quantification of migration assay. Spheroids consisting of DU145 cells or fibroblasts alone or in coculture were grown for 96 hours and placed on collagen I coated surface. The migration shown as area covered by cells was followed for 96 hours with Incucyte Zoom B, Representative images and quantification of invasion assay. Spheroids consisting of DU145 cells or fibroblasts alone or in coculture were grown for 96 hours and placed on collagen I coated surface, covered with collagen I gel and cell invasion into gel was followed for 96 hours with Incucyte Zoom. C, Representative confocal microscopy images of invasion assay at 0 and 24 hour time point. DU145 cells (green), fibroblasts (red) alone or in coculture indicate that DU145 cells move actively out from spheroids and fibroblasts tend to stay still. The treatment of cells with hydroxyl urea to inhibit cell proliferation (D) and the treatment of cells with ascorbic acid to induce the synthesis of cells own triple helical collagen (E) indicated that the observed differences were not influenced by proliferation of cells nor due to synthesis of own matrix [Color figure can be viewed at wileyonlinelibrary.com]

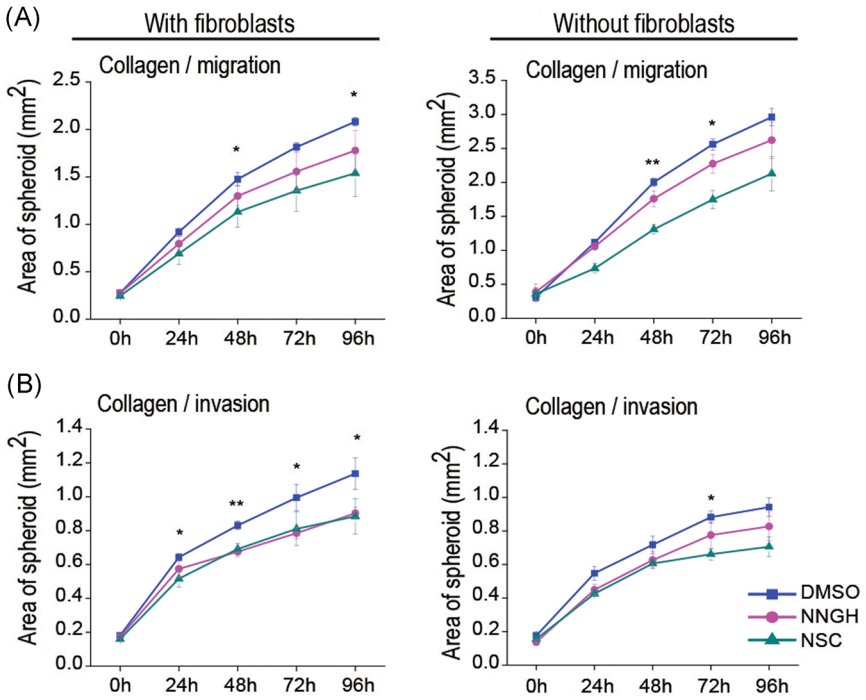

FIGURE 7 MMP inhibitors decrease the cell migration and invasion capability. A, Quantification of cell migration in the presence of MMP inhibitor NNGH and MMP-14 specific inhibitor NSC 405020. DU145 cells grown alone or with fibroblasts as spheroids for 96 hours were placed on collagen I coated surface. Cells were covered with media containing 1 μM of NNGH or 10 μM NSC405020 or DMSO as control. Migration of cells was followed for 96 hours. B, For invasion assay spheroids were covered with collagen I gel and media containing 1 μM of NNGH or 10 μM NSC405020 or DMSO as control. Invasion of cells was followed for 96 hours. DMSO, dimethyl sulfoxide; MMP, metalloproteinase [Color figure can be viewed at wileyonlinelibrary.com]

Biobank. Maria Tuominen is acknowledged for excellent technical assistance. We also thank the Proteomics and the Cell Imaging and Cytometry core facilities, supported by Biocenter Finland.

CONFLICT OF INTERESTS

The authors declare that there are no conflict of interests.

ORCID

Pekka Rappu http://orcid.org/0000-0002-5068-2842
Elina Siljamäki http://orcid.org/0000-0003-1709-8633
Jyrki Heino http://orcid.org/0000-0003-2978-805X

REFERENCES

1. Balkwill FR, Capasso M, Hagemann T. The tumor microenvironment at a glance. *J Cell Sci*. 2012;125(23):5591-5596.
2. Erler JT, Weaver VM. Three-dimensional context regulation of metastasis. *Clin Exp Metastasis*. 2009;26(1):35-49.
3. Kalluri R, Zeisberg M. Fibroblasts in cancer. *Nat Rev Cancer*. 2006;6(5):392-401.
4. Tuxhorn JA, Ayala GE, Smith MJ, Smith VC, Dang TD, Rowley DR. Reactive stroma in human prostate cancer: induction of myofibroblast phenotype and extracellular matrix remodeling. *Clin Cancer Res*. 2002;8:9-23.
5. Wen S, Hou Y, Fu L, et al. Cancer-associated fibroblast (CAF)-derived IL32 promotes breast cancer cell invasion and metastasis via integrin β3–p38 MAPK signalling. *Cancer Lett*. 2019;442:320-332.
6. Erdogan B, Webb DJ. Cancer-associated fibroblasts modulate growth factor signaling and extracellular matrix remodeling to regulate tumor metastasis. *Biochem Soc Trans*. 2017;45(1):229-236.
7. Erdogan B, Ao M, White LM, et al. Cancer-associated fibroblasts promote directional cancer cell migration by aligning fibronectin. *J Cell Biol*. 2017;216(11):3799-3816.
8. Attieh Y, Clark AG, Grass C, et al. Cancer-associated fibroblasts lead tumor invasion through integrin-β3-dependent fibronectin assembly. *J Cell Biol*. 2017;216(11):3509-3520.
9. Glentis A, Oertle P, Mariani P, et al. Cancer-associated fibroblasts induce metalloprotease-independent cancer cell invasion of the basement membrane. *Nat Commun*. 2017;8(1):924.
10. Hasebe T, Sasaki S, Imoto S, Ochiai A. Highly proliferative fibroblasts forming fibrotic focus govern metastasis of invasive ductal carcinoma of the breast. *Mod Pathol*. 2001;14(4):325-337.
11. Naba A, Clauser KR, Lamar JM, Carr SA, Hynes RO. Extracellular matrix signatures of human mammary carcinoma identify novel metastasis promoters. *eLife*. 2014;2014(3):1-23.
12. Bauer M, Su G, Casper C, He R, Rehrauer W, Friedl A. Heterogeneity of gene expression in stromal fibroblasts of human breast carcinomas and normal breast. *Oncogene*. 2010;29(12):1732-1740.
13. Nam J-M, Onodera Y, Bissell MJ, Park CC. Breast cancer cells in three-dimensional culture display an enhanced radioresponse after coordinate targeting of integrin alpha5beta1 and fibronectin. *Cancer Res*. 2010;70(13):5238-5248.
14. Sethi T, Rintoul RC, Moore SM, et al. Extracellular matrix proteins protect small cell lung cancer cells against apoptosis: a mechanism for small cell lung cancer growth and drug resistance in vivo. *Nat Med*. 1999;5(6):662-668.

15. Miyamoto H, Murakami T, Tsuchida K, Sugino H, Miyake H, Tashiro S. Tumor-stroma interaction of human pancreatic cancer: acquired resistance to anticancer drugs and proliferation regulation is dependent on extracellular matrix proteins. *Pancreas*. 2004;28(1):38-44.
16. Thomas F, Holly JMP, Persad R, Bahl A, Perks CM. Fibronectin confers survival against chemotherapeutic agents but not against radiotherapy in DU145 prostate cancer cells: involvement of the insulin like growth factor-1 receptor. *Prostate*. 2010;70(8):856-865.
17. Bix G, Iozzo RV. Matrix revolutions: 'tails' of basement-membrane components with angiostatic functions. *Trends Cell Biol*. 2005;15(1):52-60.
18. Kaukonen R, Mai A, Georgiadou M, et al. Normal stroma suppresses cancer cell proliferation via mechanosensitive regulation of JMJD1a-mediated transcription. *Nat Commun*. 2016;7:12237.
19. Olumi AF, Grossfeld GD, Hayward SW, Carroll PR, Tlsty TD, Cunha GR. Carcinoma-associated fibroblasts direct tumor progression of initiated human prostatic epithelium. *Cancer Res*. 1999;59(19):5002-5011.
20. Özdemir BC, Pentcheva-Hoang T, Carstens JL, et al. Depletion of carcinoma-associated fibroblasts and fibrosis induces immunosuppression and accelerates pancreas cancer with reduced survival. *Cancer Cell*. 2014;25(6):719-734.
21. Ojalill M, Rappu P, Siljamäki E, Taimen P, Boström P, Heino J. The composition of prostate core matrisome in vivo and in vitro unveiled by mass spectrometric analysis. *Prostate*. 2018;78:8-594.
22. Felbor U, Dreier L, Bryant RA, Ploegh HL, Olsen BR, Mothes W. Secreted cathepsin L generates endostatin from collagen XVIII. *EMBO J*. 2000;19(6):1187-1194.
23. Webber MM, Bello D, Quader S. Immortalized and tumorigenic adult human prostatic epithelial cell lines: characteristics and applications part 2. Tumorigenic cell lines. *Prostate*. 1997;30(1):58-64.
24. Ojalill M, Parikainen M, Rappu P, et al. Integrin α2β1 decelerates proliferation, but promotes survival and invasion of prostate cancer cells. *Oncotarget*. 2018;9(65):32435-32447.
25. Nagle RB, Hao J, Knox JD, Dalkin BL, Clark V, Cress AE. Expression of hemidesmosomal and extracellular matrix proteins by normal and malignant human prostate tissue. *Am J Pathol*. 1995;146(6):1498-1507.
26. Stewart DA, Cooper CR, Sikes RA. Changes in extracellular matrix (ECM) and ECM-associated proteins in the metastatic progression of prostate cancer. *Reprod Biol Endocrinol*. 2004;2:2.
27. Hao J, Jackson L, Calaluce R, McDaniel K, Dalkin BL, Nagle RB. Investigation into the mechanism of the loss of laminin 5 (alpha3beta3gamma2) expression in prostate cancer. *Am J Pathol*. 2001;158(3):1129-1135.
28. Siljamäki E, Rappu P, Riihilä P, Nissinen L, Kähäri V-M, Heino J. H-Ras activation and fibroblast-induced TGF-β signaling promote laminin-332 accumulation and invasion in cutaneous squamous cell carcinoma. *Matrix Biol*. 2019;87:26-47.
29. Moul JW, Friedrichs PA, Lance RS, Theune SM, Chang EH. Infrequent RAS oncogene mutations in human prostate cancer. *Prostate*. 1992;20(4):327-338.
30. Tsuruta D, Kobayashi H, Imanishi H, Sugawara K, Ishii M, Jones JCR. Laminin-332-integrin interaction: a target for cancer therapy? *Curr Med Chem*. 2008;15(20):1968-1975.
31. O'Reilly MS, Boehm T, Shing Y, et al. Endostatin: an endogenous inhibitor of angiogenesis and tumor growth. *Cell*. 1997;88:277-285.
32. Wickström SA, Veikkola T, Rehn M, Pihlajaniemi T, Alitalo K, Keski-Oja J. Endostatin-induced modulation of plasminogen activation with concomitant loss of focal adhesions and actin stress fibers in cultured human endothelial cells. *Cancer Res*. 2001;61:6511-6516.
33. te Velde EA, Reijerkerk A, Brandsma D, et al. Early endostatin treatment inhibits metastatic seeding of murine colorectal cancer cells in the liver and their adhesion to endothelial cells. *Br J Cancer*. 2005;92(4):729-735.
34. Ni Q, Ji H, Zhao Z, Fan X, Xu C. Endostar, a modified endostatin inhibits non small cell lung cancer cell in vitro invasion through osteopontin-related mechanism. *Eur J Pharmacol*. 2009;614(1-3):1-6.
35. Wickström SA, Alitalo K, Keski-Oja J. Endostatin associates with lipid rafts and induces reorganization of the actin cytoskeleton via down-regulation of RhoA activity. *J Biol Chem*. 2003;278(39):37895-37901.
36. Liu X, Nie W, Xie Q, et al. Endostatin reverses immunosuppression of the tumor microenvironment in lung carcinoma. *Oncol Lett*. 2018;15(2):1874-1880.
37. Lee JH, Isayeva T, Larson MR, et al. Endostatin: a novel inhibitor of androgen receptor function in prostate cancer. *Proc Natl Acad Sci U S A*. 2015;112(5):1392-1397.
38. Chang J-H, Javier JAD, Chang G-Y, Oliveira HB, Azar DT. Functional characterization of neostatins, the MMP-derived, enzymatic cleavage products of type XVIII collagen. *FEBS Lett*. 2005;579(17):3601-3606.
39. Olson OC, Joyce JA. Cysteine cathepsin proteases: regulators of cancer progression and therapeutic response. *Nat Rev Cancer*. 2015;15(12):712-729.
40. Olsen J, Kirkeby LT, Brorsson MM, et al. Converging signals synergistically activate the LAMC2 promoter and lead to accumulation of the laminin gamma2 chain in human colon carcinoma cells. *Biochem J*. 2003;371(1):211-221.

SUPPORTING INFORMATION

Additional supporting information may be found online in the Supporting Information section.

How to cite this article: Ojalill M, Virtanen N, Rappu P, Siljamäki E, Taimen P, Heino J. Interaction between prostate cancer cells and prostate fibroblasts promotes accumulation and proteolytic processing of basement membrane proteins. *The Prostate*. 2020;80:715–726. https://doi.org/10.1002/pros.23985